

DEVELOPMENT OF A MOVING AND STATIONARY MIXED PARTICLE METHOD FOR SOLVING THE INCOMPRESSIBLE NAVIER-STOKES EQUATIONS AT HIGH REYNOLDS NUMBERS

Chinlong Huang¹ and Tony W. H. Sheu^{1,2,3}

5

¹*Department of Engineering Science and Ocean Engineering,
National Taiwan University, Taipei, Taiwan, Republic of China*

²*Taida Institute of Mathematical Science (TIMS), National Taiwan
University, Taipei, Taiwan, Republic of China*

³*Center for Advanced Studies in Theoretical Sciences (CASTS),
National Taiwan University, Taipei, Taiwan, Republic of China*

10

In the current particle method, we propose a new semi-implicit particle method for more effectively solving the incompressible Navier-Stokes equations at a high Reynolds number. Within the Lagrangian framework, the convective terms in the equations of motion are eliminated, without the problem of convective numerical instability. Also, the crosswind diffusion error generated normally in the case of a large angle difference between the velocity vector and the coordinate line disappears. Only the Laplacian operator for the velocity components and the gradient operator for the pressure need to be approximated on the basis of particle interaction through the currently proposed kernel function. As the key to getting better predicted accuracy, the kernel function is derived subject to theoretical constraint conditions. In the conventional moving-particle method, it is almost impossible to get convergent solution at a high Reynolds number. To overcome this simulation difficulty so that the moving-particle method is applicable to a wider range of flow simulations, a new solution algorithm is proposed for solving the elliptic-parabolic set of partial differential equations. In the momentum equations, calculation of the velocity components is carried out in the particle-moving sense. Unlike the traditional moving-particle semi-implicit method, the pressure values are not calculated at the particle locations being advected along the flow-field. After updating the fluid particle locations within the Lagrangian framework, we interpolate the velocities at uniformly distributed pressure locations. In the current semi-implicit solution algorithm, pressure is governed by the elliptic differential equation with the source term being contributed entirely to the velocity gradient terms. The distribution of particle locations can become highly nonuniform in cases involving a high Reynolds number and under conditions having an apparently vortical flow. As a result, the elliptic nature of the pressure can be considerably destroyed in the course of Lagrangian motion. To retain the embedded ellipticity in the incompressible viscous flow equations, the Poisson equation adopted for the calculation of pressure is solved in a mathematically more plausible fixed uniform mesh so as to get not only fourth-order accuracy for the pressure but also to enhance ellipticity in the pressure Poisson equation. Moreover, the velocity–pressure coupling can be more enhanced in the semi-implicit solution algorithm. The proposed moving and stationary mixed particle semi-implicit solution algorithm and the particle kernel will be

15

20

25

30

35

40

Received 3 March 2012; accepted 2 April 2012.

Address correspondence to Tony W. H. Sheu, No. 1, Sec. 4, Roosevelt Road, Taipei, 10617, Taiwan, Republic of China. E-mail: twhsheu@ntu.edu.tw.

NOMENCLATURE

d number of dimensions	u velocity component in the x direction
f dependent variable	v velocity component in the y direction
h distance between two particles	w kernel function
i, j particle indices	δ delta function
n^0 particle number density	ν kinematic viscosity
g gravitational acceleration	ρ density
r particle location	ϕ scalar function
r_e radius of a small circle	

demonstrated to be suitable to simulate high-Reynolds number fluid flows by investigating the lid-driven cavity flow problem at $Re = 100$ and $Re = 1,000$. Besides the validation of the proposed semi-implicit particle method in the fixed domain, the broken-dam problem is also solved to demonstrate the ability of accurately capturing the time-evolving free surface using the proposed semi-implicit particle method.

45

1. INTRODUCTION

Numerical methods developed for performing flow simulations can be divided into three major classes, Eulerian, Lagrangian, and mixed Eulerian/Lagrangian. In the Eulerian class of numerical methods, flow equations are solved for a fixed mesh system. On the other hand, in the Lagrangian class of numerical methods, which can be further subdivided into two subgroups, mesh-based and mesh-free, either the mesh points or the fluid particles are allowed to advect with the fluid flow. As a result of permitting the particles to move in the Lagrangian sense, we no longer need to approximate these convective terms in the transport equations. The resulting avoidance of approximating the convective terms and thus the elimination of numerical instability terms turns out to be one of the apparent advantages of employing the Lagrangian approach in flow simulations. Numerical errors of the cross-wind diffusion type can also be well eliminated. Another mathematically rigorous arbitrary Lagrangian-Eulerian (ALE) method [1] involves using both the Lagrangian and Eulerian solution steps in the course of moving the mesh points from one time to another.

Several well-known grid-based methods such as the marker-and-cell (MAC) [2], volume-of-fluid (VOF) [3], and level-set [4] methods have been developed to predict free surface flows. Another class of mesh-free methods known as the particle methods was developed on the basis of the prescribed particles being allowed to move in the Lagrangian sense. As a result, approximation of the convective terms can be avoided without incurring any numerical instability and thus generating diffusion error. Particle methods are separated into the Eulerian particle method, such as the particle-in-cell (PIC) method [5], and the Lagrangian particle methods, which include the smoothed particle hydrodynamics (SPH) and the moving-particle semi-implicit (MPS) meshless types. The SPH method was first introduced by Lucy [6] and Gingold and Monaghan [7] in 1977 in their simulation of compressible fluid flows. The SPH method was developed on the basis of interpolation theory through

the use of a kernel function (or smoothing kernel). This method was later extended to simulate incompressible free-surface flow [8].

75

The moving-particle semi-implicit gridless method was recently developed to simulate incompressible Navier-Stokes fluid flows [9]. The particle method is based on the interaction of each reference particle with its neighboring particles by means of the kernel (or weight) function. All the spatial derivatives can be calculated solely by means of the deterministic particle interaction, without the need to generate a mesh in the flow. The freedom of allowing particles to advect with the fluid without the cost of a time-consuming mesh generation explains why the MPS method has gradually become effective for use in simulating many practical problems involving either complicated geometry or complex physics. For flow problems investigated at a higher Reynolds number, this method, however, has difficulty getting a convergent solution [10, 11]. In addition, the MPS method has been blamed for a deterioration accuracy of when increasing the number of particles. These two numerical drawbacks motivate the present formulation of the moving and stationary mixed particle method.

80

85

The rest of this article is organized as follows. In Section 2 the Navier-Stokes equations for predicting the incompressible fluid flow are presented. In Section 3, the new interaction kernel is presented for the approximation of the gradient and Laplacian differential terms. This is followed by presentation of the solution algorithm formulated within a moving mesh framework for the momentum equations and a stationary mesh framework for the pressure Poisson equation. In Section 4 our emphasis is on the derivation of the kernel function used in the present particle method. In Section 5, the proposed particle method is validated by solving the analytical, lid-driven cavity and dam-break problems at low as well as high Reynolds numbers. In Section 6, conclusions are drawn based on the predicted results.

90

95

2. WORKING EQUATIONS

100

The following Navier-Stokes equations for the motion of an incompressible fluid flow will be considered in a simply connected domain Ω .

$$\frac{D\mathbf{u}}{Dt} = -\frac{1}{\rho}\nabla p + \nu\nabla^2\mathbf{u} + \mathbf{q} \quad (1)$$

$$\frac{1}{\rho}\frac{D\rho}{Dt} = -\nabla \cdot \mathbf{u} \quad (2)$$

where

105

$$\frac{Dg}{Dt} = \frac{\partial g}{\partial t} + (\mathbf{u} \cdot \nabla)g \quad (3)$$

Note that $g = \mathbf{u}$ in (1) and $g = \rho$ in (2). In the above momentum equations, ρ stands for the density of the fluid, ν for the kinematic viscosity, and \mathbf{q} for the gravitational acceleration vector.

110

3. DEVELOPMENT OF THE KERNEL FUNCTION FOR THE SPATIAL DIFFERENTIAL OPERATORS

In comparison with the grid-based methods, particle-based methods have gradually become popular for simulating the incompressible Navier-Stokes equations that are subject to either a free surface or an interface. In particle methods, one needs to transform the differential operators shown in the mass and momentum conservation equations to their corresponding particle interaction operators. In other words, Eqs. (1–2) written in the continuous differential context are transformed to their corresponding discrete particle interaction context. The transport equations under current investigation can then be approximated by the chosen moving particles and their interaction. The success of applying a particle method depends on the kernel (or weighting) function chosen for the particles that are distanced from each other by the user's prescribed finite length for the approximation of the incompressible flow velocity vectors and the pressure around these particles.

Given a particle at which its physical quantity f_i is defined at a position r_i . The value of f_i can be approximated as follows by virtue of the employed kernel function $w(\mathbf{r})$:

$$\langle f(\mathbf{r}) \rangle \cdot \sum_i w(|\mathbf{r}_i - \mathbf{r}|) = \sum_i f_i w(|\mathbf{r}_i - \mathbf{r}|) \quad (4)$$

In the above equation, the smoothed quantity $\langle f \rangle_i$ for f at the point r_i is exactly identical to the local value of f_i provided that the kernel function shown in (4) is chosen as the Dirac delta function. This implies that the chosen kernel function $w(\mathbf{r})$, which should be constrained by the integral constraint equation $\int_V w(r) dV = 1$, determines the simulation quality using the particle method. Different kernel functions have been discussed in [12].

For a scalar at an arbitrary interior location r_j , its value ϕ_j can be expanded in Taylor series with respect to the value of ϕ at r_i as follows:

$$\phi_j = \phi_i + \nabla \phi|_{ij} \cdot (\mathbf{r}_j - \mathbf{r}_i) + \text{H.O.T.} \quad (5)$$

By neglecting the higher-order terms (H.O.T.) shown above, the first-order approximated equation $\phi_j - \phi_i = \nabla \phi|_{ij} \cdot (\mathbf{r}_j - \mathbf{r}_i)$ is obtained. Multiplication of $(\mathbf{r}_j - \mathbf{r}_i)^{-1}$ on both sides of the resulting simplified Taylor series expansion equation yields

$$\nabla \phi|_{ij} = \frac{(\phi_j - \phi_i)(\mathbf{r}_j - \mathbf{r}_i)}{|\mathbf{r}_j - \mathbf{r}_i| |\mathbf{r}_j - \mathbf{r}_i|} \quad (6)$$

Let $\nabla \phi|_{ij}$ be f and substitute it into Eq. (4). This substitution enables us to get the following smoothed representation of $\nabla \phi$, which is denoted by $\langle \nabla \phi \rangle$, at the node ij in a domain of $d (= 2)$ dimension

$$\langle \nabla \phi \rangle|_{ij} = \frac{d}{n_i} \sum_{j \neq i} \frac{\phi_j - \phi_i}{|\mathbf{r}_j - \mathbf{r}_i|} (\mathbf{r}_j - \mathbf{r}_i) w(\mathbf{r}_j - \mathbf{r}_i) \quad (7)$$

In the above, $n_i = \left(\sum_{j \neq i} w(|\mathbf{r}_j - \mathbf{r}_i|) \right)$ denotes the particle number density. Under the incompressible flow condition, n_i is equal to the initial value of the particle number density n^0 .

The following Laplacian operator applied to a scalar function ϕ can be similarly derived as [9]

155

$$\langle \nabla^2 \phi \rangle_i = \frac{2d}{\lambda n^0} \sum_{j \neq i} (\phi_j - \phi_i) w(|\mathbf{r}_j - \mathbf{r}_i|) \quad (8)$$

where

$$\lambda = \frac{\int_{V'} |\mathbf{r}_j - \mathbf{r}_i|^2 w(|\mathbf{r}_j - \mathbf{r}_i|) dV}{\int_{V'} w(|\mathbf{r}_j - \mathbf{r}_i|) dV} \quad (9)$$

Note that V' shown above is the volume that is excluded of a small interval containing the point at i . One can also have the freedom to employ the following Laplacian operator given in [13]:

160

$$\langle \nabla^2 \phi \rangle_{ij} = \frac{2d}{n^0} \sum_{j \neq i} \frac{\phi_j - \phi_i}{|\mathbf{r}_j - \mathbf{r}_i|^2} w(|\mathbf{r}_j - \mathbf{r}_i|) \quad (10)$$

It is now easy to see the advantage of applying the particle method, since all the spatial derivatives can be calculated solely from the kernel function without the need to generate a time-consuming mesh in the physical domain. Much of the computational effort needed to generate a good-quality mesh for performing an accurate numerical simulation in a domain possibly involving moving boundaries is therefore avoided. Note also that calculations of the values of $\nabla \phi$ and $\nabla^2 \phi$ by Eqs. (7), (8), and (10) involve using only the kernel function $w(\mathbf{r})$ rather than employing the derivative of kernel function as used in the SPH particle method. As a result, we have greater flexibility to choose the kernel function, which may have a slope as steep as the Dirac delta function.

165

170

4. DEVELOPMENT OF THE PROPOSED KERNEL FUNCTIONS

175

According to Eqs. (7) and (8–10), the quality of approximating the operators $\langle \nabla \phi \rangle_{ij}$ and $\langle \nabla^2 \phi \rangle_i$ is known to depend very much on the chosen kernel function $w(\mathbf{r})$ and the number of the user's prescribed particles. Moreover, where to place the particles and what kind of kernel function is used determine the subsequent particle locations in a moving fashion. For this reason, the chosen kernel function will be derived below in detail.

180

The Dirac delta function $\delta(\mathbf{r})$, which is shown in (4) and is constrained by $\int_{-\infty}^{\infty} \delta(\mathbf{r}) d\mathbf{r} = 1$, is a mathematically rigorous kernel function. This ideal function is unfortunately not implementable in computational practice, and we have to resort to its corresponding smoothed delta function so as to be able to carry out flow simulations based on the particle method. The smoothed function is sometimes called the nascent delta function $\delta_\varepsilon(\mathbf{r})$, which is defined as $\varepsilon \xrightarrow{\lim} 0 \delta_\varepsilon(\mathbf{r}) = \delta(\mathbf{r})$. Other nascent

185

delta functions such as the Gaussian function, Lorentz line function, impulse function, and sinc function can be found in the literature. One can also use other kinds of kernel function which were developed irrelevantly to the nascent delta functions. 190
The exponential, cubic spline and quadratic spline, functions proposed by Belytschko et al. [14] and the kernel functions proposed by Koshizuka and Oka [15] and Koshizuka et al. [16] are three typical examples.

The kernel function $w(\underline{r})$ under current development follows the mathematical identity given by $r_e \xrightarrow{\text{lim}} 0 w(\underline{r}, r_e) = \delta(\underline{r})$, where r_e is the radius of a small circle. 195
The weight between any two particles that are a distance r apart from each other become negligibly small as $r \geq r_e$. Also, for the sake of accuracy, the kernel function will be developed to retain the following constraint condition in the Dirac delta function:

$$\int_{-\infty}^{\infty} w(\underline{r}, r_e) d\underline{r} = 1 \quad (11)$$

The proposed kernel function will be represented in terms of the dimensionless length r/r_e as follows

$$w(r) = \begin{cases} \frac{a}{r_e} + \frac{b}{r_e} \left(\frac{r}{r_e}\right) + \frac{c}{r_e} \left(\frac{r}{r_e}\right)^2 + \frac{d}{r_e} \left(\frac{r}{r_e}\right)^3 + \frac{e}{r_e} \left(\frac{r}{r_e}\right)^4 & 0 \leq r \leq r_e \\ 0 & r_e < r \end{cases} \quad (12)$$

205

By imposing the constraint conditions given by $w(r=r_e) = (\partial w/\partial r)|_{r=r_e} = (\partial w/\partial r)|_{r=0} = 0$ and $\int_0^{r/r_e=1} w(r) dr = \frac{1}{2}$, the algebraic equations given below can be derived

$$a + b + c + d + e = 0 \quad (13)$$

$$b + 2c + 3d + 4e = 0 \quad (14)$$

$$a + \frac{b}{2} + \frac{c}{3} + \frac{d}{4} + \frac{e}{5} = \frac{1}{2} \quad (15)$$

$$b = 0 \quad (16)$$

By solving the above four algebraic equations, one can easily express the coefficients a , b , c , d in terms of e as $a = 1 - (1/15)e$, $b = 0$, $c = -3 + (6/5)e$, 215
 $d = 2 - (32/15)e$.

We will develop the kernel function for $\nabla^2 p$, where p represents the pressure, in the uniform mesh. The reason is that in the incompressible flow simulation the pressure Poisson equation will be solved in a stationary grid so as to be able to properly simulate a higher-Reynolds-number incompressible fluid flow within the semi-implicit framework. A similar viewpoint was also mentioned previously in [10, 11]. 220
By substituting the resulting kernel function into Eq. (10) for $\phi(=p)$, the corresponding discrete equation for the Laplace equation, $(\partial^2 p/\partial x^2) + (\partial^2 p/\partial y^2) = 0$ can be

derived using the proposed particle kernel:

$$\frac{\partial^2 p}{\partial x^2} + \frac{\partial^2 p}{\partial y^2} = \frac{1}{[w(h) + 2w(\sqrt{2}h)]h^2} [(p_{i+1,j} + p_{i-1,j} + p_{i,j+1} + p_{i,j-1} - 4p_i)w(h) + (p_{i+1,j+1} + p_{i-1,j+1} + p_{i+1,j-1} + p_{i-1,j-1} - 4p_i)w(\sqrt{2}h)] \quad (17)$$

Through the modified equation analysis performed on the above equation, the modified equation can be derived as

$$\begin{aligned} \frac{\partial^2 p}{\partial x^2} + \frac{\partial^2 p}{\partial y^2} = & - \left[\frac{w(\sqrt{2}h)}{w(h) + 2w(\sqrt{2}h)} \frac{\partial^4 p}{\partial x^2 \partial y^2} + \frac{1}{12} \frac{\partial^4 p}{\partial x^4} + \frac{1}{12} \frac{\partial^4 p}{\partial y^4} \right] h^2 \\ & - \left\{ \frac{w(\sqrt{2}h)}{12(w(h) + 2w(\sqrt{2}h))} \left(\frac{\partial^6 p}{\partial x^4 \partial y^2} + \frac{\partial^6 p}{\partial x^2 \partial y^4} \right) \right. \\ & \left. + \frac{1}{360} \frac{\partial^6 p}{\partial x^6} + \frac{1}{360} \frac{\partial^6 p}{\partial y^6} \right\} h^4 + \dots \end{aligned} \quad (18)$$

230

It is worthy of note that the first term on the right-hand side of (18) becomes zero provided that $w(\sqrt{2}h) = \frac{1}{4}w(h)$ [17].

When choosing $r_e = 2h$, where h denotes the grid size, the nine-point discrete equation (17) has fourth-order accuracy under the condition

$$3a + \left(2\sqrt{2} - \frac{1}{2}\right)b + \left(2 - \frac{1}{4}\right)c + \left(\sqrt{2} - \frac{1}{8}\right)d + \left(1 - \frac{1}{16}\right)e = 0 \quad (19)$$

The resulting five free parameters can then be uniquely determined from Eqs. (13)–(16) and (19) as

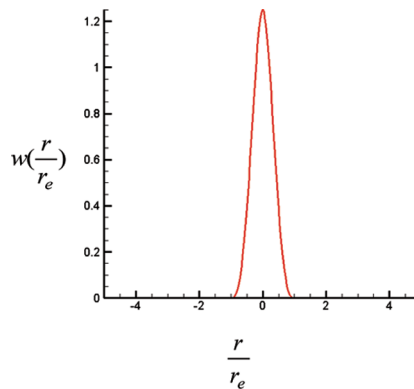
$$\begin{aligned} a &= \frac{480\sqrt{2} - 705}{512\sqrt{2} - 745} & b &= 0 & c &= \frac{-960\sqrt{2} + 1515}{512\sqrt{2} - 745} & d &= \frac{-210}{512\sqrt{2} - 745} \\ e &= \frac{480\sqrt{2} - 600}{512\sqrt{2} - 745} \end{aligned}$$

5. MOVING AND STATIONARY MIXED PARTICLE SOLUTION ALGORITHM

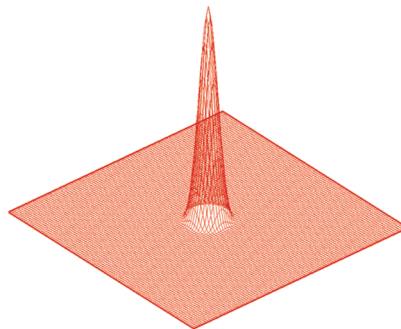
While the MPS method is an effective method to predict complex flow physics in a time-varying domain, this method is applicable only to a very-low-Reynolds-number flow simulation. For this reason, we are motivated to extend the MPS method so that it can be applicable to predict a higher-Reynolds-number flow. Revision of the traditional MPS method so as to solve the elliptic-parabolic equations at high Reynolds numbers is based on the splitting of the solution algorithm into two steps. In the first advection step, the velocity solutions are computed explicitly from the momentum equations using the moving-particle method without

invoking the approximation of the advective spatial operator. This eliminates both of the numerical problems of convective instability and the erroneous false diffusion error that is normally encountered in the Eulerian formulation. Upon obtaining the new particle locations and the updated particle number density, we proceed to compute the pressure from the pressure Poisson equation implicitly, based on the currently available velocity values for the calculation of the source term on the right-hand side of the equation.

In contrast to the conventional MPS method, in the current semi-implicit solution algorithm, the pressure values are not calculated at the velocity locations. All the pressure solutions computed from the pressure Poisson equation are at uniformly redistributed locations. The underlying idea of not solving the pressure at the same locations as the velocity components is that moving particles become non-uniformly distributed in the vortical flow simulation. This is particularly serious in the case of high Reynolds numbers. As a result of the nonuniformly distributed particle locations, the elliptic nature of the Poisson equation will be poorly simulated. This motivates us to solve the pressure Poisson equation at regular mesh points rather than at the particle locations that are changed from time to time in a Lagrangian sense. In this light, the velocity components computed from the momentum equations will be



(a)



(b)

Q2 **Figure 1.** Proposed kernel function plotted (a) against r/r_e ; (b) in xy plane (color figure available online).

interpolated to their values at the regular pressure nodes. With the computed pressure values at the regular mesh points, we can get first the velocity correction values and then the corrected velocities at the nonuniformly distributed particle locations through interpolation. This completes the calculation of the primitive variables (\underline{u} , p). A detailed flowchart of the proposed moving and stationary mixed particle semi-implicit solution algorithm is shown schematically in Figure 2.

6. NUMERICAL RESULTS

6.1. Analytical Incompressible Navier-Stokes Problems

Q1 The developed kernel function will be employed first to solve the analytical incompressible Navier-Stokes equations for the sake of validating the proposed kernel function.

$$u \frac{\partial u}{\partial x} + v \frac{\partial u}{\partial y} = -\frac{\partial p}{\partial x} + \frac{\partial}{\partial x} \left(\frac{1}{\text{Re}} \frac{\partial u}{\partial x} \right) + \frac{\partial}{\partial y} \left(\frac{1}{\text{Re}} \frac{\partial u}{\partial y} \right) \quad (20)$$

$$u \frac{\partial v}{\partial x} + v \frac{\partial v}{\partial y} = -\frac{\partial p}{\partial y} + \frac{\partial}{\partial x} \left(\frac{1}{\text{Re}} \frac{\partial v}{\partial x} \right) + \frac{\partial}{\partial y} \left(\frac{1}{\text{Re}} \frac{\partial v}{\partial y} \right) \quad (21)$$

$$\frac{\partial u}{\partial x} + \frac{\partial v}{\partial y} = 0 \quad (22)$$

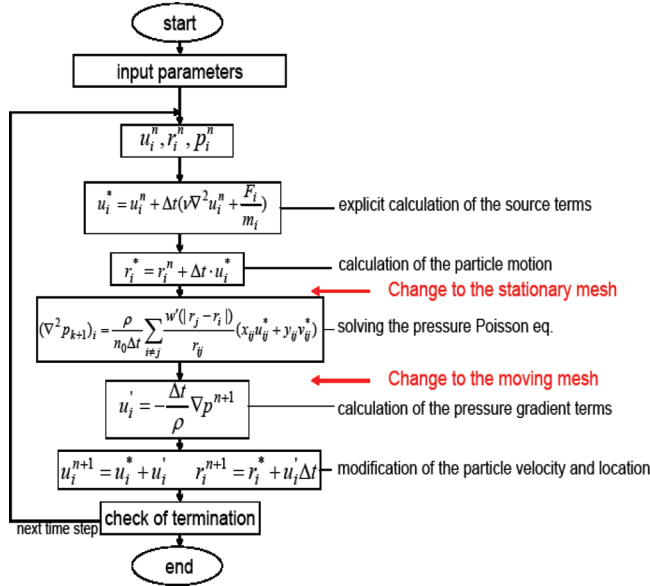


Figure 2. Flowchart of proposed moving and stationary mixed particle method (color figure available online).

Table 1. Predicted L_2 -error norms and corresponding rates of convergence for the Navier-Stokes equations

Mesh	L_2 -error norm of u	Rate of convergence
11×11	9.307×10^{-5}	
21×21	2.161×10^{-5}	2.10662
31×31	1.012×10^{-5}	1.87104
41×41	5.865×10^{-6}	1.89623

where $Re = UL/\nu$ stands for the Reynolds number. The following problem, which is amenable to analytic solution in a square domain of unit length, will be investigated. The exact pressure for Eqs. (20–22) takes the form

285

$$p = \frac{-2}{(1+x)^2 + (1+y)^2} \quad (23)$$

provided that the boundary velocities are specified analytically according to the exact velocities given below:

$$u = \frac{-2(1+y)}{(1+x)^2 + (1+y)^2} \quad (24)$$

$$v = \frac{2(1+x)}{(1+x)^2 + (1+y)^2} \quad (25)$$

At different meshes, the predicted L_2 -error norms and their corresponding spatial rates of convergence, shown in Table 1, justify the newly proposed particle method.

We then solve the second problem, which is also amenable to analytic solution, given by

295

$$u = 1 - e^{\lambda x} \cos(2\pi y) \quad (26)$$

$$v = \frac{\lambda}{2\pi} e^{\lambda x} \sin(2\pi y) \quad (27)$$

$$p = \frac{1}{2}(1 - e^{2\lambda x}) \quad (28)$$

Table 2. L_2 -error norms and corresponding rates of convergence predicted at $Re = 1,000$ in different meshes

Mesh	L_2 -error norm of u	Rates of convergence
11×11	1.082×10^{-3}	
21×21	6.948×10^{-5}	3.96096
31×31	1.603×10^{-5}	3.61702
41×41	6.756×10^{-6}	3.00342

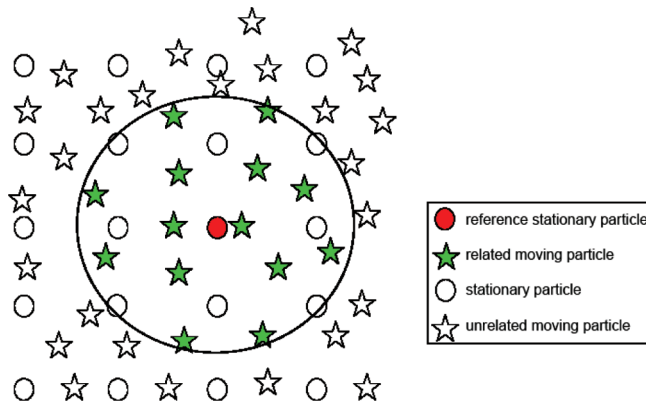


Figure 3. Schematic of interpolation from the moving particles to the reference stationary particle (color figure available online).

In this study, the value of λ is chosen to be $\lambda = \text{Re}/2 - \sqrt{\text{Re}^2/4 + 4\pi^2}$. For the calculation carried out at $\text{Re} = 1,000$, the L_2 -error norms predicted in four meshes and their corresponding rates of convergence are tabulated in Table 2. 300

6.2. Dam-Break Problem

The investigated dam-break problem is shown schematically in Figure 4, where L ($=1$) denotes the height and the width of stillwater, in the tank. The computed results were compared with the results given in [18]. Figures 5a–5f show the results of the fluid flow investigated at $\text{Re} = 500$. Figures 6a–6f are the results predicted at $\text{Re} = 47,000$. The red lines denote the simulated free surfaces, and they agree very well with those shown in [18]. 305

6.3. High-Re Lid-Driven Cavity Flow Problem

The final example to be investigated is known as the lid-driven cavity problem, whose solution has been well documented in the literature. In the past, this problem received a great deal of attention because of its geometric simplicity and physical complexity. The boundary velocities u and v are assumed to be zero everywhere 310



Figure 4. Schematic of the investigated dam-break problem.

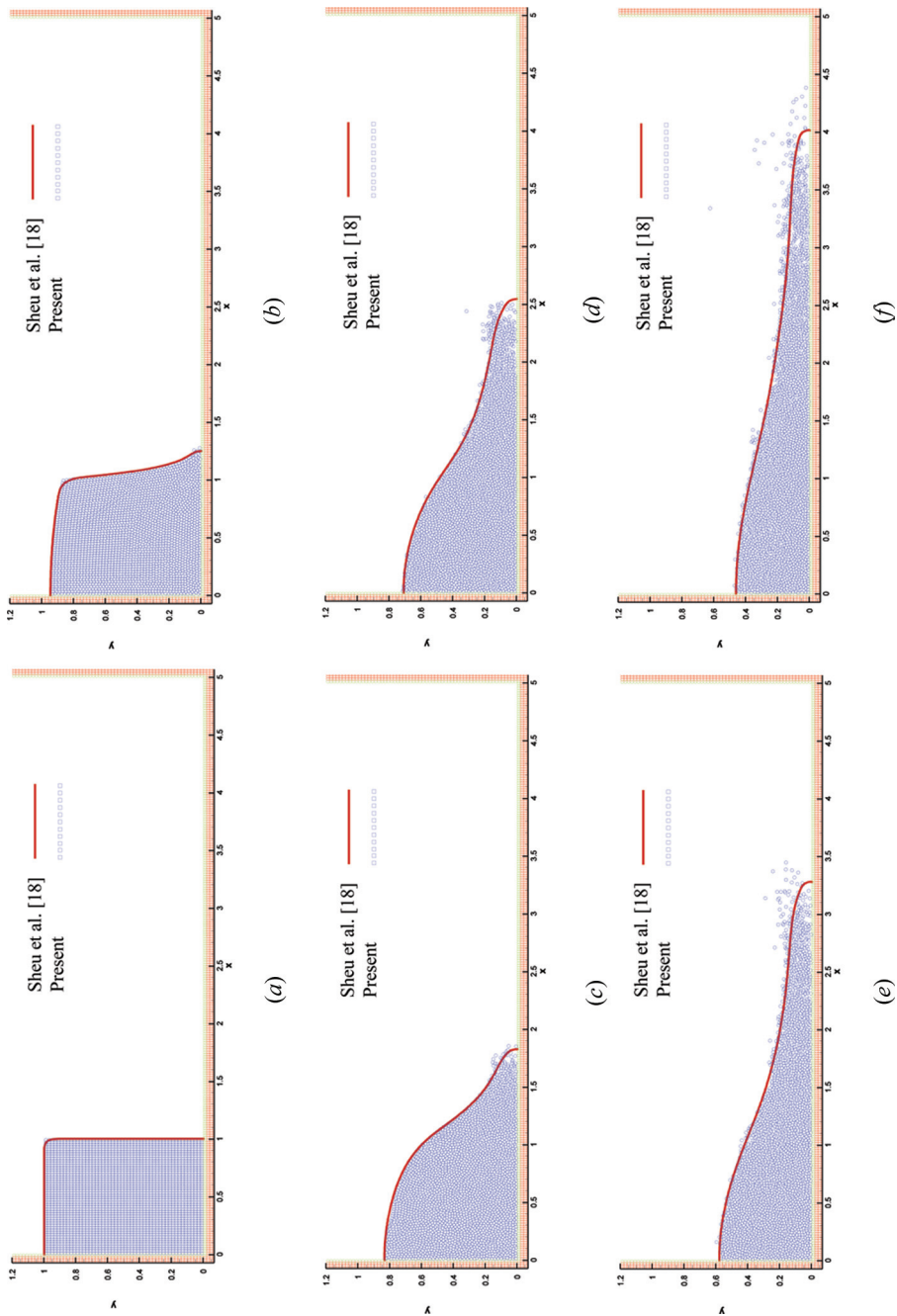


Figure 5. Comparison of the predicted free surfaces using the proposed particle method and the level set method at different times for the case with $Re = 500$: (a) $t = 0.0$; (b) $t = 1.0$; (c) $t = 1.5$; (d) $t = 2.0$; (e) $t = 2.5$; (f) $t = 3.0$ (color figure available online).

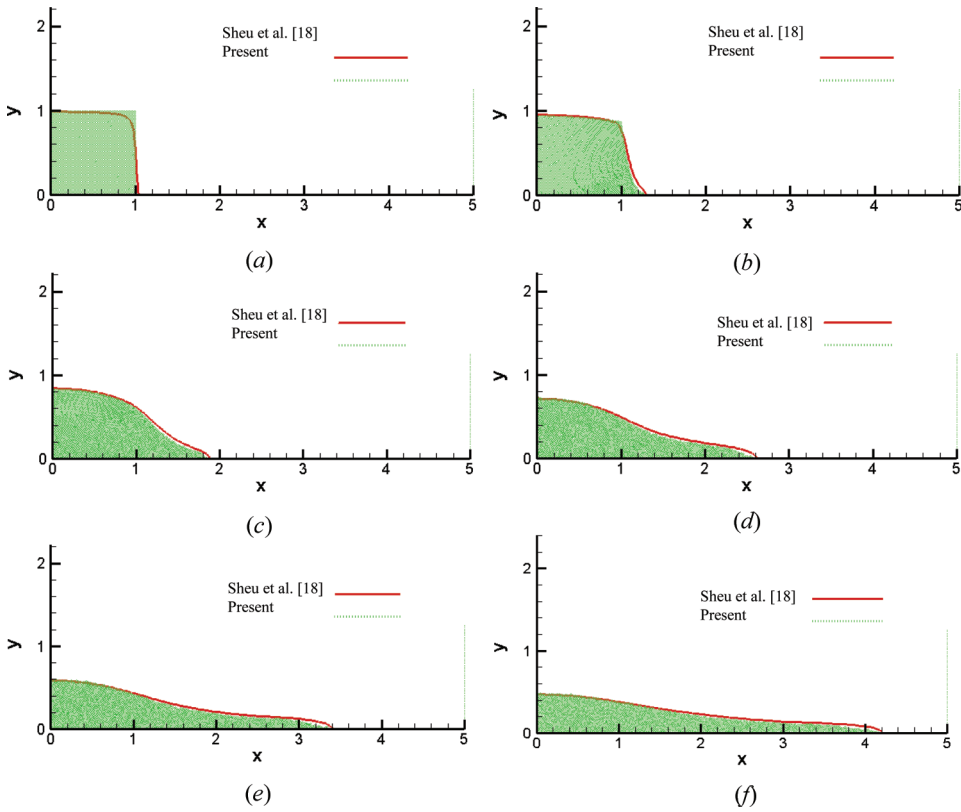


Figure 6. Comparison of the predicted free surfaces using the proposed particle method and the level set method at different times for the case with $Re = 47,000$: (a) $t = 0.0$; (b) $t = 0.5$; (c) $t = 1.0$; (d) $t = 1.5$; (e) $t = 2.0$; (f) $t = 2.5$ (color figure available online).

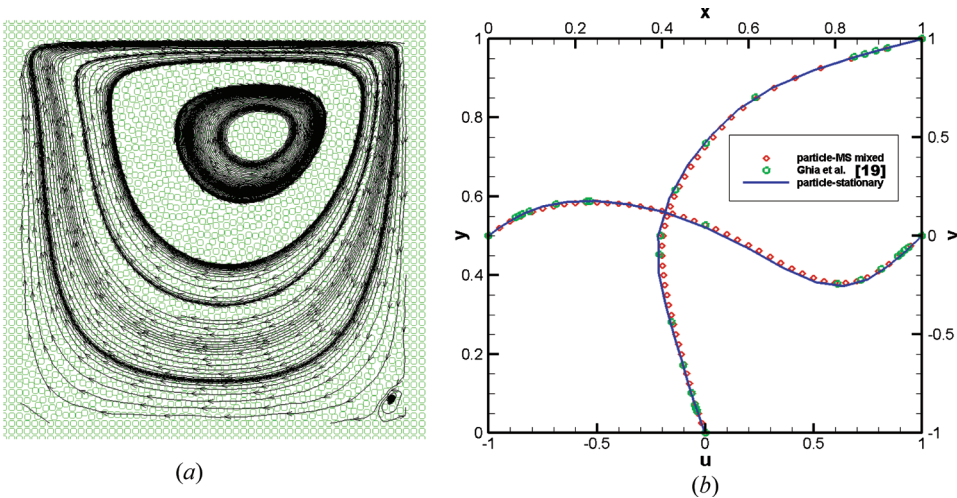


Figure 7. (a) Particle distribution at steady state. (b) Comparison of the predicted and referenced velocity profiles of u at $x = 0.5$ and v at $y = 0.5$ for the case investigated at $Re = 100$ (color figure available online).

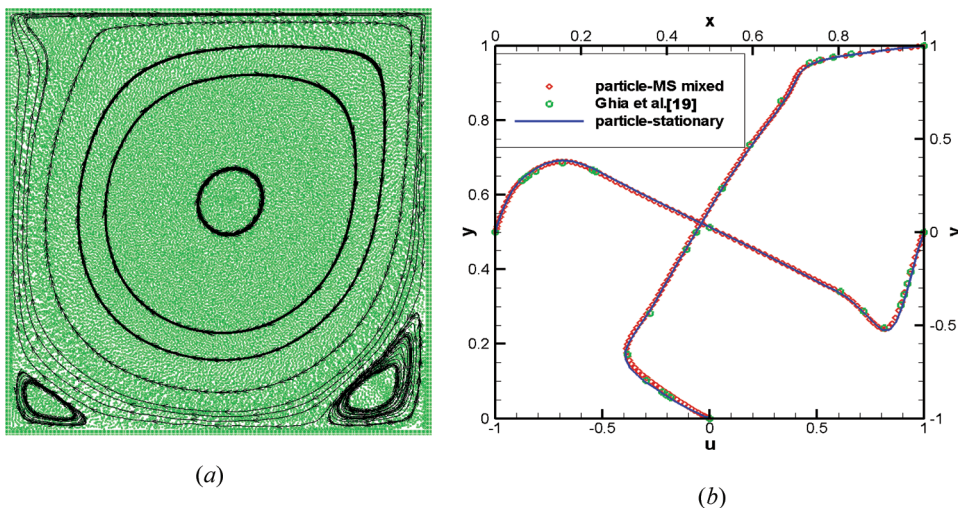


Figure 8. (a) Particle distribution at steady state. (b) Comparison of the predicted and referenced velocity profiles of u at $x=0.5$ and v at $y=0.5$ for the case investigated at $Re=1,000$ (color figure available online).

except at the points along the top boundary, where $u=1$ and $v=0$. Calculations are performed at Reynolds numbers 100 and 1,000 in meshes containing 51×51 and 201×201 nodal points, respectively. 315

For the sake of comparison, the results computed at two Reynolds numbers are plotted along the mid-sectional horizontal and vertical lines in Figures 7 and 8, respectively. The present results are seen to compare very well with the finite-difference solutions of Ghia et al. [19]. 320

7. CONCLUDING REMARKS

This article has developed a new particle method for the calculation of the incompressible Navier-Stokes equations at high Reynolds numbers in a semi-implicit sense. When approximating the momentum equations, only the Laplacian and gradient differential operators are involved for the velocity components. Calculation of the pressure values from the Poisson equation also involves the Laplacian operator. It is essential to develop a kernel function for the Laplacian operator in a rigorous sense within the framework of the moving and stationary particle method. In addition, for the pressure Poisson equation this kernel function yields fourth-order spatial accuracy in the fixed uniform mesh. Note that the pressure Poisson equation is solved in an uniform stationary mesh while the momentum equations are predicted in the moving sense. The reason for the calculation of the primitive variables \underline{u} and p in different meshes is to get a high-Re convergent solution using the moving and stationary mixed particle semi-implicit method. Since different meshes are invoked for the velocity and pressure unknowns, interpolation of the velocity itself and the velocity correction between two meshes is needed so as to be able to retain the elliptic nature of the pressure Poisson equation. Through the analysis of the analytical and two benchmark problems, known as the lid-driven cavity and broken-dam problems, 325 330 335

the proposed kernel function, which is developed to get a fast convergent pressure solution, and the newly proposed mixed particle method carried out in two meshes, are both demonstrated to be correct when solving incompressible viscous flow equations at high Reynolds numbers. 340

REFERENCES

1. C. W. Hirt, A. A. Amsden, and J. L. Cook, An Arbitrary Lagrangian-Eulerian Computing Method for All Flow Speeds, *J. Comput. Phys.*, vol. 14, pp. 227–253, 1974. 345
2. F. H. Harlow and J. E. Welch, Numerical Calculation of Time-Dependent Viscous Incompressible Flow of Fluid with a Free Surface, *Phys. Fluids*, vol. 8, pp. 2182–2189, 1965.
3. C. W. Hirt and B. D. Nichols, Volume of Fluid (VOF) Method for Dynamics of Free Boundaries, *J. Comput. Phys.*, vol. 39, pp. 201–221, 1981. 350
4. S. Osher and R. P. Fedkiw, Level Set Methods: An Overview and Some Recent Results, *J. Comput. Phys.*, vol. 169–2, pp. 463–502, 2001.
5. F. H. Harlow, A Machine Calculation Method for Hydrodynamic Problems, *Los Alamos Sci. Lab. Report LAMS-1956*, 1955.
6. L. B. Lucy, A Numerical Approach to the Testing of the Fission Hypothesis, *Astr. J.*, vol. 82, pp. 1013–1024, 1977. 355
7. R. R. Gingold and J. J. Monaghan, Smoothed Particle Hydrodynamics: Theory and Application to Non-Spherical Stars, *Astr. J.*, vol. 181, pp. 375–389, 1977.
8. J. J. Monaghan, Simulating Free Surface Flows with SPH, *J. Comput. Phys.*, vol. 110, pp. 399–406, 1994. 360
9. S. Koshizuka, H. Tamako, and Y. Oka, A Particle Method for Incompressible Viscous Flow with Fluid Fragmentation, *CFD J.*, vol. 4, pp. 29–46, 1995.
10. Y. H. Hwang, A Moving Particle Method with Embedded Pressure Mesh (MPPM) for Incompressible Flow Calculation, *Numer. Heat Transfer B*, vol. 60, pp. 370–398, 2011.
11. Y. H. Hwang, Smoothing Difference Scheme in a Moving Particle Method, *Numer. Heat Transfer B*, vol. 60, pp. 203–234, 2011. 365
12. B. Ataie-Ashtiani and L. Farhadi, A Stable Moving-Particle Semi-Implicit Method for Free Surface Flows, *Fluid Dyn. Res.*, vol. 38, pp. 241–256, 2006.
13. S. Zhang, K. Morita, K. Fukuda, and N. Shirakawa, An Improved MPS Method for Numerical Simulations of Convective Heat Transfer Problems, *Int. J. Numer. Meth. Fluids*, vol. 51, pp. 31–47, 2006. 370
14. T. Belytschko, Y. Krongaux, D. Organ, M. Fleming, and P. Krysz, Meshless Methods: An Overview and Recent Developments, *Comput. Meth. Appl. Mech. Eng.*, vol. 139, pp. 3–47, 1996.
15. S. Koshizuka and Y. Oka, Moving-Particle Semi-implicit Method for Fragmentation of Incompressible Fluids, *Nucl. Sci. Eng.*, vol. 123, pp. 421–434, 1996. 375
16. S. Kohizuka, A. Nobe, and Y. Oka, Numerical Analysis of Breaking Waves Using the Moving Particle Semi-implicit Method, *Int. J. Numer. Meth. Fluids*, vol. 26, pp. 751–769, 1998.
17. C. L. Huang, T. W. H. Sheu, T. Ishikawa, and T. Yamaguchi, Development of a Particle Interaction Kernel for Convection-Diffusion Scalar Transport Equation, *Numer. Heat Transfer B*, vol. 60, pp. 96–115, 2011. 380
18. T. W. H. Sheu, C. H. Yu, and P. H. Chiu, Development of a Dispersively Accurate Conservative Level Set Scheme for Capturing Interface in Two-Phase Flows, *J. Comput. Phys.*, vol. 228, pp. 661–686, 2009.
19. U. Ghia, K. N. Ghia, and C. T. Shin, High-Re Solutions for Incompressible Flow Using the Navier-Stokes Equations and a Multigrid Method, *J. Comput. Phys.*, vol. 48, pp. 387–411, 1982. 385